

This item is the archived peer-reviewed author-version of:

Baseline findings in the Retrospective Digital Computer Analysis of Keratoconus Evolution (REDCAKE) Project

Reference:

Jiménez-García Marta, Ní Dhubhghaill Siorcha, Koppen Carina, Varssano David, Rozema Jos.- Baseline findings in the Retrospective Digital Computer Analysis of Keratoconus Evolution (REDCAKE) Project
Cornea - ISSN 0277-3740 - 40:2(2021), p. 156-167
Full text (Publisher's DOI): <https://doi.org/10.1097/ICO.0000000000002389>
To cite this reference: <https://hdl.handle.net/10067/1715530151162165141>

Baseline findings in Retrospective Digital Computer Analysis of Keratoconus Evolution (REDCAKE) project.

Marta Jiménez-García, MSc ^{a,b} (<https://orcid.org/0000-0002-2839-9696>)

Sorcha Ní Dhubhghaill, MD, PhD ^{a,b} (<https://orcid.org/0000-0002-1115-7834>)

Carina Koppen, MD, PhD ^{a,b} (<https://orcid.org/0000-0002-7728-7260>)

David Varssano, MD^{c,*} (<https://orcid.org/0000-0002-1704-8145>)

Jos J. Rozema, PhD ^{a,b,*} (<https://orcid.org/0000-0001-8124-8646>)

The REDCAKE Study Group

- a. *Department of Ophthalmology, Antwerp University Hospital (UZA), Edegem, Belgium*
- b. *Department of Medicine and Health Sciences, University of Antwerp, Antwerp, Belgium*
- c. *Department of Ophthalmology, Tel Aviv Sourasky Medical Center, Tel Aviv, Israel affiliated with the Sackler Faculty of Medicine, Tel Aviv University, Tel Aviv, Israel*

* These authors share senior authorship

Corresponding Authors:

Marta Jiménez-García,

Department of Ophthalmology, Antwerp University Hospital, Wilrijkstraat 10, 2650 Edegem, (Belgium)

Phone Number: +32 3 265 2556 (marta.jimenez.garcia@outlook.com)

Jos Rozema

Department of Ophthalmology, Antwerp University Hospital, Wilrijkstraat 10, 2650 Edegem, (Belgium)

Phone Number: +32 3 265 2556 (Jos.Rozema@uza.be)

Keywords:

keratoconus; corneal tomography; keratoconus location; keratoconus asymmetry; keratoconus progression;

Conflicts of Interest and Source of Funding: An awarded Flemish Grant (FWO-TBM 000416N) provided financial support for this study. The authors declare no conflicts of interest.

ABSTRACT

Purpose

To present the baseline data for a large cohort of keratoconus patients enrolled in the Retrospective Digital Computer Analysis of Keratoconus Evolution (REDCAKE) study.

Methods

Eight centers contributed Scheimpflug tomographical data for 906 keratoconus patients, 743 measured with a Pentacam and 163 with a Galilei. The stage of keratoconus at baseline, the location of the reference points, minimum pachymetry (P_{\min}), and maximum keratometry (K_{\max}) were analyzed. The inter-eye asymmetry was evaluated for K_{\max} (anterior and posterior), P_{\min} and keratoconus stage. Average maps and elevation profiles were calculated for each degree of keratoconus.

Results

Keratoconus was more frequently diagnosed in males (73%) than in females (27%). At baseline, 500/1155 eyes (43%) presented with moderate to severe changes in the posterior surface; while moderate/severe changes were only found in 252 and 63 eyes when evaluating anterior surface and pachymetry respectively. The location of P_{\min} was usually inferotemporal (94% OD and 94% OS), while the location of K_{\max} showed more variability and significantly higher distance from apex ($p < 0.05$). The keratoconus presentation was chiefly asymmetric for all the parameters studied. Clear differences between stages could be identified in the maps and elevation profiles.

Conclusion

The staging map set presented can be used as a graphical guidance to classify keratoconus stage. Keratoconus presented asymmetrically, and generally the posterior surface was more affected than the anterior surface or the thickness. Asymmetry is playing a role in KC detection. While P_{\min} was almost invariably located inferotemporally, K_{\max} location showed higher variability and distance from the apex.

INTRODUCTION

Keratoconus (KC) is an ectatic corneal disease¹ characterized by a progressive thinning and protrusion of the cornea.² This cascade of events occurring in the cornea is usually associated with increasing irregular astigmatism and myopia, whereas the axial length in keratoconic eyes remains similar to healthy controls.³ The onset of the disease is typically during puberty² and a wide range of prevalence and incidence rates have been reported, probably influenced by the diagnostic tools available at the time. A recent nation-wide study in the Netherlands showed a prevalence of 1:375, with an annual incidence of 13.3 new cases per 100,000 in the 10-40 years old group.⁴

While the etiology of KC remains unexplained, key risk factors such as atopy,⁵ mechanical trauma (rubbing),⁶ genetic^{7,8} and environmental factors⁹ play major roles in KC genesis. The disease is typically bilateral, although often asymmetric in both time and severity,^{10,11} even to the point that one eye may appear normal. It is widely accepted that purely unilateral KC does not exist,¹ and the normal appearing “form fruste” corneas are likely to show signs of KC in the long-term follow-up.^{12,13} The contralateral eye with normal topography of a patient with KC, is considered therefore the earliest and mildest form of the disease.¹⁴

KC is progressive but even without intervention, the progression will normally stop during the third or the fourth decade of life.² The damage accrued over time, however, may be severely visually disabling and may require corneal transplantation. Fortunately, current management strategies,¹⁵ including early detection, regular monitoring, the use of specialty contact lenses and the appearance of stabilizing treatments to prevent KC progression, have reduced the number of patients proceeding to transplantation.¹⁶⁻¹⁸ One landmark treatment is corneal cross-linking (CXL), which can effectively stabilize the cornea, although it requires evidence demonstrating the presence of such progression.¹⁹

Defining progression and KC stage remains a challenge due to the variable nature of both keratoconic and normal corneas. New assessment techniques and parameters are available, based on e.g. elevation, thickness profiles, corneal aberrometry or biomechanics that may assist with those definitions.²⁰⁻²² Progression has already been associated with high anterior and posterior keratometry, corneal astigmatism, inferior-superior asymmetry, progression in the contralateral eye, asymmetric topography patterns, back elevation, coma aberration and higher levels of cortisol.^{1,12,23-28} Younger age at the time of detection is also a highly significant risk factor for faster progressive KC.^{16,26,29,30} In addition, the biomechanical properties of the corneal tissue can be influenced by hormonal changes

in pregnancy, or undergoing in-vitro fertilization treatment,^{31,32} placing these women at risk of ectasia progression.

Despite the ongoing efforts of the scientific community, there is no widely accepted consensus on KC progression.³³ The purpose of this study is to report the baseline characteristics of the patients enrolled in the Retrospective Digital Computer Analysis of Keratoconus Evolution study (REDCAKE), a retrospective multicenter observational study that aims to create new diagnostic tools for early detection and risk assessment of KC progression. This work represents the first part of the largest, longitudinal topography analysis of keratoconic corneas since the '90s using current, state-of-the-art technology.

MATERIALS AND METHODS

Tomographic and demographic data was provided by eight member sites of EVICR.net (European Vision Institute Clinical Research Network), a network of European ophthalmological sites that performs multinational clinical research in ophthalmology. These sites were the University Medical Centre of Johannes Gutenberg-University and Justus Liebig University Giessen (Germany), Ghent and Antwerp University Hospitals, both in Belgium, Fondation Asile des Aveugles - Hôpital Ophtalmique Jules Gonin (Switzerland), University Eye Clinic Maastricht (The Netherlands), Hospital de Braga (Portugal) and Tel Aviv Sourasky Medical Centre (Israel). Keratoconic patient data with two or more corneal tomographies at least 5 months apart were collected to form the REDCAKE dataset. The REDCAKE study was designed and carried out in compliance with the tenets of the Declaration of Helsinki and it was registered in the clinical trials database clinicaltrials.gov (identification no. NCT03235856). Voluntary informed consent was obtained from all the patients according to local laws and ethical approval was granted from the Institutional Review Board of all the participating centers for the revision of the medical files and clinical examinations.

Data collection was performed retrospectively, based on the inspection of corneal tomographer databases and medical files, considering the inclusion and exclusion criteria specified in Table 1. The patients were diagnosed in tertiary centers by a cornea specialist according to the habitual criteria (corneal steeping, inferior/superior asymmetry, corneal thinning, slit lamp signs such as Vogt striae, etc.) supplemented by the information provided by the latest upgrades available at the time of diagnosis, such as thickness profiles or Belin-Ambrósio Display.

Table 1. Inclusion and exclusion criteria

Inclusion criteria:

- *Clinically diagnosed KC in one or both eyes*
 - *Age between 12–40 years*
 - *Two or more Scheimpflug tomographies (Pentacam, Galilei) of good technical quality, separated at least five months apart*
-

Exclusion Criteria:

- *Corneal scarring present in the study eye(s)*
 - *Ocular comorbidities*
 - *Ocular surgeries/ treatments (including crosslinking) before or between measurements.*
 - *Known systemic diseases (e.g. diabetes, multiple sclerosis, etc.), except allergies*
 - *Known change in contact lenses between measurements*
 - *Fluorescein drops instilled into the eye before Scheimpflug measurement.*
-

Seven centers provided Pentacam tomographies (Oculus Optikgeräte GmbH, Germany), which were processed using a recent version of the analysis software (version 6.08r30) to access all available parameters. The last remaining center provided Galilei tomographies (Ziemer Ophthalmic Systems AG, Port, Switzerland) as comma separated values (.csv) files, allowing analyses of the axial and tangential curvature maps from the anterior and posterior cornea, anterior and posterior elevation using different reference surfaces, as well as the pachymetry.

In the Pentacam group, only measurements with an ‘OK’ quality score designation (82.5%), as well as measurements with minor errors (marked yellow; 17.5%) were included. Although measurements marked in yellow should be interpreted with caution, accepting those examinations allowed inclusion of the more severe cases, for which a perfect quality measurement could not be achieved. Galilei examinations that did not include thirteen csv files were considered incomplete and were deleted from the database. Eyes with only one remaining examination after the quality check were also excluded. This resulted in a total of 906 patients for analysis: 743 measured with Pentacam and 163 with Galilei, with a total of 3739 Pentacam examinations and 1179 examinations taken with Galilei. Here, only baseline examinations (585 OD and 570 OS measured with Pentacam and 134 OD and 128 OS measured with Galilei) were considered.

No slit-lamp examinations or best-corrected distance visual acuity (BCDVA) were collected for REDCAKE patients, so KC staging was based purely on tomographic data. A novel platform-independent classification system based on machine learning (LOGIK) was used to classify all examinations. (Submitted, Issarti et al. Logistic index for keratoconus detection and severity scoring (LOGIK)) Well-established grading systems are also reported as a reference, but these are either platform-dependent or not applicable to the entire cohort as not all required parameters are available for all patients. Pentacam offers two KC grading systems: the Topographical Keratoconus

Classification (TKC), based on a modified Amsler-Krumeich scale, and the ABCD grading system, that utilizes the thinnest pachymetry (P_{min}), as well as the anterior (ARC) and posterior (PRC) radii of curvature calculated over a 3 mm area surrounding the thinnest point, to calculate the discretized A, B and C values. Since BCDVA is not available and it is required to calculate the D value, this parameter was not considered. Meanwhile, the Galilei examinations were classified according to Amsler-Krumeich keratometry and pachymetry criteria.

Matlab R-2019b (The MathWorks Inc., Natick, MA) was used to analyze the data and SPSS 25 (SPSS, Inc., Chicago, IL) was used for statistical analysis, with an alpha of 0.05 considered the cut-off value for significance.

RESULTS

Scheimpflug examinations and demographic data were provided by eight centers. Centers designated A to H contributed Pentacam data. Centre A recruited 82 patients, center B 65 patients, center C 353 patients, center D 83, center E 92 patients, center F 45 and center H 23 patients. Finally, center I provided examinations of 163 patients measured with Galilei. More details on the patients and their examinations can be found in Table 2.

		PENTACAM GROUP	GALILEI GROUP
Examinations period		Nov.2006- Dec.2018	Jan. 2011 and Jul. 2017
Patients (N=906)	Both eyes examined	412	99
	Only OD examined	173	35
	Only OS examined	158	29
	TOTAL	743	163
Eyes (N=1417)	OD	585	134
	OS	570	128
	TOTAL	1155	262
Follow-up period	Min.	5 months	5 months
	Max	10.5 years	6.5 years
	<36 months	790 eyes	219 eyes
	>36 months	365 eyes	43 eyes

DEMOGRAPHIC DATA

The REDCAKE cohort comprises 906 patients clinically diagnosed with KC, 657 of whom were men (73%) and 249 women (27%). All of them were diagnosed in tertiary centers by a cornea specialist. The mean age at baseline was 26.6 ± 6.6 years. Ninety-four patients (78 measured with Pentacam

and 16 measured with Galilei) were between 12 and 18 years old, and those will be considered the pediatric KC subgroup. At least 23 of them were under 15 when the disease was detected. Out of the 721 patients with a reported ethnicity, 538 were Caucasian (75%), 172 Middle-Eastern/ North African (24%), 7 African (<1%) and 4 Asian (<1%). While Middle-Eastern/ North African represented an 11% of the Pentacam group they represented the 68% of the Galilei group.

The descriptive statistics of the Pentacam and Galilei data are shown in Table 3. Given the differences between both devices in terms of available parameters and the structural peculiarities of the data, both groups were treated separately in some of the analyses. The elevation and curvature maps were considered sufficiently similar to allow a joint analysis focused on calculating average profiles.

Table 3. Descriptive statistics at baseline. (Mean± SD [95%Confidence Interval]).

DEVICE	Age (yrs)	K _{max} (D)		P _{min} (μm)	
		OD*	OS*	OD	OS
Pentacam	26.74±6.57 [26.26-27.21]	53.04±7.20 [52.45-53.62]	52.52±6.17 [52.01-53.03]	471.74±44.70 [468.11-475.37]	474.63±41.50 [471.22-478.04]
Galilei	25.74±6.52 [24.74-26.75]	54.19±9.33 [52.60-55.79]	55.27±17.34 [52.23-58.30]	470.37±66.57 [458.99-481.74]	465.94±94.09 [449.48-482.40]
		Max elev. anterior 4 mm (μm)		Max elev. posterior 4 mm (μm)	
DEVICE		OD	OS	OD	OS
Pentacam		24.62±15.31 [23.38-25.86]	23.70±13.62 [22.58-24.82]	48.90±26.82 [46.72-51.07]	48.35±24.37 [46.34-50.35]
Galilei		23.08±15.27 [20.47-25.69]	22.30±17.21 [19.29-25.31]	47.66±30.61 [42.43-52.89]	43.69±27.52 [38.88-48.51]
		Ant. elev. thinnest point (μm)		Post. elev. thinnest point (μm)	
DEVICE		OD	OS	OD	OS
Pentacam		20.15±14.50 [18.97-21.33]	19.38±12.53 [18.35-20.41]	43.46±27.68 [41.21-45.71]	43.07±25.25 [40.99-45.15]
Galilei		17.76±14.50 [15.28-20.24]	16.19±13.15 [13.89-18.49]	43.28±35.55 [37.20-49.35]	42.73±49.15 [34.13-51.32]

* Pentacam: N=585 OD and 570 OS. Galilei N=134 OD and 128 OS

KC STAGE

In the Pentacam group, 163 eyes (14%) were misclassified as normal by TKC (false negatives), 11 eyes (1%) were considered abnormal or post-refractive surgery ectasia and 43 (4%) were considered KC suspect. The rest were assigned to a KC stage ranging from stage 1 to 4, being KC 2 the stage with the highest prevalence at baseline (Table 4).

TKC CLASSIFICATION	OD	OS	TOTAL
-	88	75	163
Poss.	21	22	43
KC 1	57	69	126
KC 1-2	55	52	107
KC 2	136	137	273
KC 2-3	60	74	134
KC 3	104	83	187
KC 3-4	53	52	105
KC 4	6	0	6
Abnormal, post-surgery, etc.	5	6	11
TOTAL:	585	570	1155

Based on the ABCD classification, 157 eyes (13.6%) were incorrectly classified as normal (A0B0C0). At baseline, 500 eyes (43%) were classified as moderate/advanced according to their posterior surface ($B \geq 3$). Meanwhile, manifest moderate ($A = 3$), advanced ($A = 4$) stages in the anterior surface were found in 252 eyes (22%), and 1092 eyes (95%) remained classified as early and mild ($C \leq 2$) according to the pachymetry criterium. On the other hand, 78 examinations (7%) showed alterations of the back surface with no changes in the thickness or the anterior surface ($A0 B > 0 C0$) and 84 eyes (7%) had abnormal pachymetry without showing alterations in curvature ($A0 B0 C > 0$). Only 2 eyes showed alterations in the anterior curvature prior to posterior and stromal changes ($A > 0 B0 C0$).

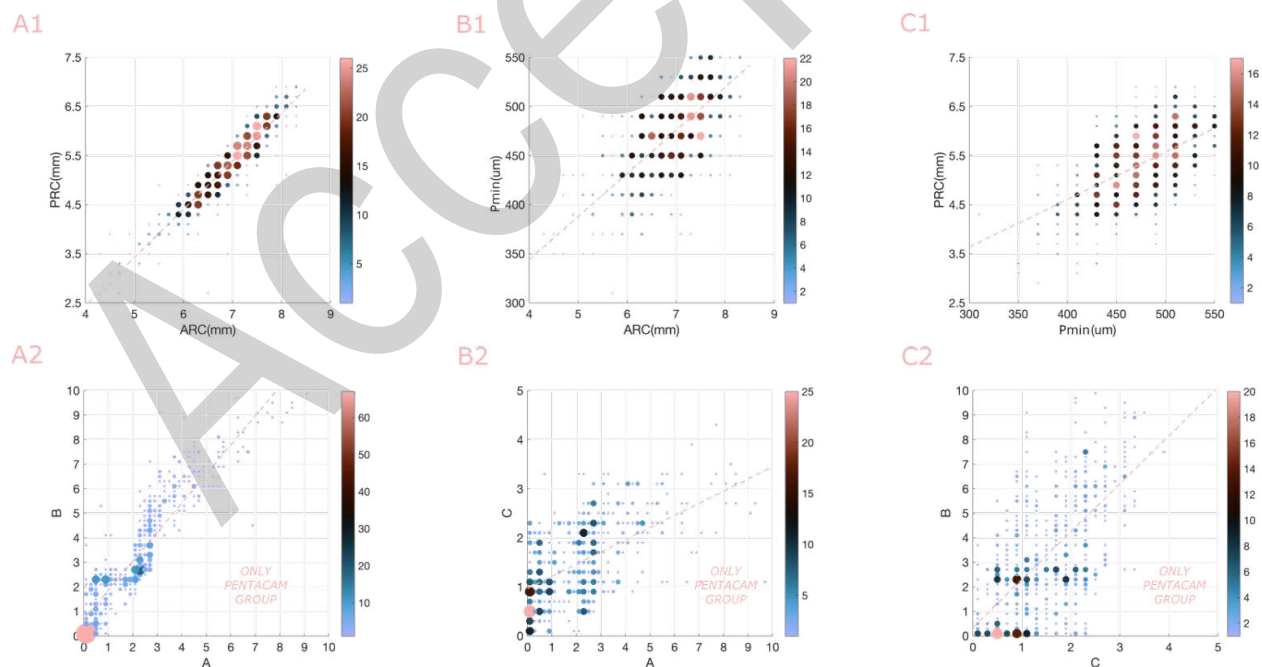


Figure 1. Comparison of KC stage at baseline. **First row:** relations between physical parameters ARC, PRC (mean anterior and posterior curvatures calculated over a 3mm area surrounding the thinnest point) and thickness at the thinnest point (P_{min}) calculated for 719 OD eyes. **Bottom row:** relations between the real values of A, B and C-proprietary ABCD classification algorithm, only Pentacam (585 OD eyes) -.

Figure 1 shows the relations between the physical parameters ARC, PRC and P_{min} (upper row), which are processed using a proprietary algorithm to produce the ABCD classification (bottom row). As shown in subplot A2, most of the values are located above the diagonal (or line x=y in C2), meaning that, at baseline, most of the eyes presented a deviation from a normal cornea more evident in the posterior surface (related to B parameter) than in the anterior surface and the pachymetry (related to A and C parameters respectively).

Table 5 shows the tomographic indices and additional descriptive values for the Pentacam group at baseline examination. No significant difference was found between OD and OS in any of the parameters included.

PARAMETER	OD (N=585)	OS (N=570)
IVA (mm)	0.84±0.53	0.81±0.47
ISV	75.93±44.02	72.23±37.78
KI	1.21±0.15	1.19±0.12
CKI	1.04±0.05	1.04±0.05
IHA (µm)	25.84±21.14	26.75±21.73
IHD (µm)	0.09±0.07	0.09±0.06
BAD-D	7.19±4.67	6.86±3.81
Rmin (mm)	6.47±0.79	6.51±0.72
ARC (mm)	6.91±0.70	6.93±0.64
PRC (mm)	5.29±0.72	5.30±0.67
ARTmin (µm)	430.45±218.36	437.98±213.10
ARTavg (µm)	294.44±121.73	296.47±119.07
ARTmax (µm)	205.15±94.18	205.44±93.10
RPImin	1.40±0.80	1.33±0.62
RPlavg	1.90±0.96	1.83±0.69
RPImax	2.81±1.47	2.73±1.14
KMaxZonalMean3mm (D)	50.87±5.85	50.52±5.00
KMaxZonalMean4mm (D)	50.59±5.67	50.24±4.88
KMaxZonalMean5mm (D)	50.02±5.33	49.72±4.63

IVA, index of vertical asymmetry; ISV, index of surface variance; KI, keratoconus index; CKI, central keratoconus index; IHA, index of height asymmetry; IHD, index of height decentration; BAD-D, Belin Ambrósio Display Deviation, Rmin, minimum radius of curvature; ARC, anterior radius of curvature in an area of 3mm surrounding the thinnest point; PRC, posterior radius of curvature in an area of 3mm surrounding the thinnest point; ART, Ambrósio relational thickness; RPI, pachymetric progression index; KMaxZonalMean, Average keratometry in an area surrounding K_{max} point of 3, 4 or 5mm.

The mean values of the tomographic indices were over the pathological limits according to the manufacturer's manual (IVA>0.32, ISV>41, KI>1.07, CKI>1.03, IHA>21, IHD>0.016).

Applying the Amsler-Krumeich scale to the Galilei examinations, 160 eyes were Stage I KC, 59 were Stage II and the rest (43 eyes) were Stage III, with average central keratometry readings greater than 53D and no central scar. Mean central keratometry in a 3 mm diameter area and minimum

pachymetry were $49.00 \pm 6.58D$ and $470.37 \pm 66.57 \mu m$ for right eyes, and $49.30 \pm 9.03D$ and $465.94 \pm 94.09 \mu m$ for left eyes. ARC, PRC and P_{min} were calculated for the Galilei group as well and included in the analysis (Figure 1, top row). PRC and ARC showed a very strong correlation (Pearson $r=0.938$ for OD, $r=0.934$ for OS $p<0.001$) according to Evans scale.³⁴ ARC and PRC were also correlated with P_{min} and the level was strong for OD ($r=0.637$ and $r=0.646$, respectively, $p<0.001$) and moderate for OS ($r=0.524$ and $r=0.510$ $p<0.001$).

Classification using LOGIK

Recently, a logistic classification system for KC severity based on machine learning (LOGIK) was presented. (Submitted, Issarti et al. Logistic index for keratoconus detection and severity scoring (LOGIK)) LOGIK classification is calculated from elevation maps and minimum pachymetry value, and therefore platform-independent. This feature allowed to classify KC in the entire REDCAKE sample. LOGIK detected 1366 eyes (96.4%) with KC, with 51 false negatives (Table 6). Since LOGIK is a continuous system and is based on a logistic function, the stage obtained is more evenly distributed than other scales.

Table 6. LOGIK classification at baseline for the entire cohort

CLASSIFICATION	LOGIK VALUES	OD	OS	TOTAL
NORMAL (FALSE NEG.)	$LOGIK \leq -0.8$	42	9	51
FORME FRUSTE	$-0.8 < LOGIK \leq 0.5$	103	109	212
EARLY	$0.5 < LOGIK \leq 1.5$	172	145	317
MILD	$1.5 < LOGIK \leq 2.5$	195	202	397
MODERATE	$2.5 < LOGIK \leq 3.5$	197	221	418
ADVANCED	$LOGIK \geq 3.5$	10	12	22
TOTAL:		719	698	1417

KERATOCONUS LOCATION

The location of P_{min} and K_{max} was examined separately for OD and OS eyes. With few exceptions, P_{min} was located in the inferotemporal quadrant for both OD (94% of eyes) and OS (94% of eyes). For OD, only 29 eyes showed an inferonasal location and superior location was found for 15 eyes. For OS, 18 thinnest points were located in the superior cornea and 27 in inferonasal positions. The cloud corresponding to the P_{min} locations is much denser than the one corresponding to K_{max} (Figure 2 -OD- and Supplemental Digital Content 1 -OS-). The position of P_{min} was mostly located within 2 mm from the corneal apex (OD: 0.92 ± 0.39 mm from apex, OS: 0.97 ± 0.38 mm), while the location of K_{max} showed a significant higher variability (OD: 1.49 ± 0.87 mm from apex, OS: 1.56 ± 0.86 mm; $p < 0.001$ in both eyes). About 90% of the K_{max} locations were inferior for OD and only 31% of them were located in the inferotemporal cornea. Similar numbers were seen for OS (92% of and 34%, respectively). The Kruskal-Wallis test followed by a Dunn- Bonferroni approach (multiple nonparametric comparisons with a

global level of significance $p < 0.05$) was performed to compare the distances from P_{min} and K_{max} to apex at different KC stages, according to LOGIK classification. For OD, the difference between groups was only significant between early and moderate KC groups for both P_{min} and K_{max} ($p < 0.05$). For OS, P_{min} showed significant difference in early vs. moderate and mild vs. moderate keratoconus. The K_{max} position, on the other hand, was significantly different in the forme fruste group compared to the false negatives group and to the early KC and in moderate KC compared to the false negatives group and the mild KC group.

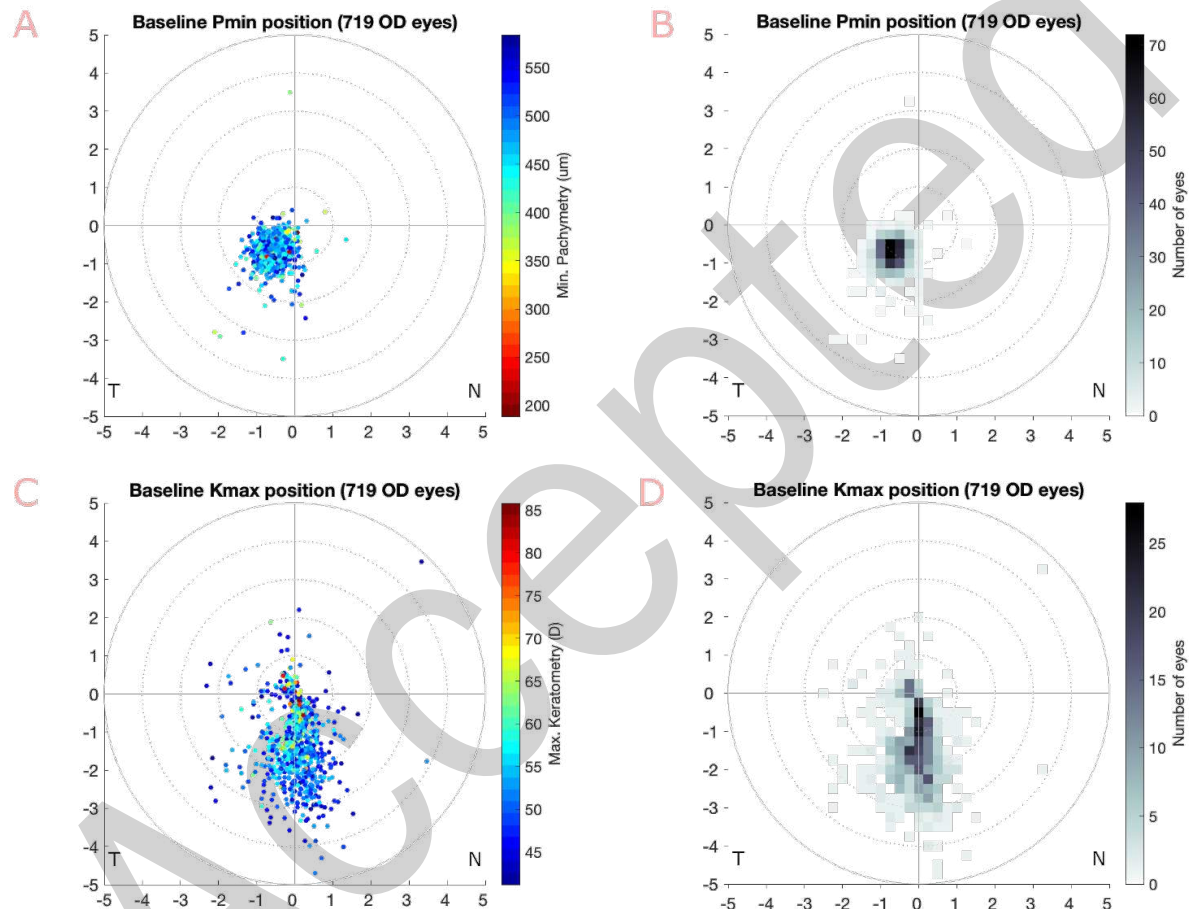


Figure 2. Minimum corneal pachymetry (P_{min}) and maximum anterior keratometry (K_{max}) at baseline examination for 719 OD eyes. Axes: distance from corneal center (mm) **A.** Location of P_{min} . Colour scale related to pachymetry value. **B.** Frequency heatmap graph for the location of P_{min} . **C.** Location of K_{max} . Color scale related to keratometry value. **D.** Frequency heatmap graph for the location of K_{max} . OS graphs can be found as Supplemental Digital Content file A.

KERATOCONUS ASYMMETRY

The inter-eye asymmetry on the severity of KC was evaluated for some of the most common descriptive parameters. Minimum pachymetry (P_{min}), maximum anterior keratometry (K_{max}), minimum posterior

radius and LOGIK analysis was performed using data of both Pentacam and Galilei groups (511 patients), while only the 412 Pentacam patients were considered for TKC and BAD-D asymmetry, both calculated with proprietary algorithms. For each patient, the best (least affected) and the worst (most affected) eye were independently defined for each parameter. The eye with the lowest value for LOGIK, K_{max} , TKC and BAD-D parameters was considered the best eye, while the eyes with the lowest P_{min} and the lowest posterior radius (steeper) were considered the worst. 78% of eyes were uniformly classified as best eye or worst eye for all parameters studied.

In the graphs (Figure 3) the size of the bubbles is proportional to the frequency of the corresponding pair (best eye level, worst eye level). Plots include the diagonal as a reference for equality in severity and colors represent the magnitude of the difference between eyes. For plotting purposes, eyes classified as abnormal for TKC ($n = 11$) were not considered in the TKC graph, while those with TKC = '-' were assigned a numeric value of 0 and those with TKC = 'poss.' a value of 0.5. Intermediate stages KC 1-2, KC 2-3 etc. were considered as 1.5, 2.5 etc. For continuous variables (LOGIK, K_{max} anterior, K_{max} posterior, P_{min} and BAD-D), measurements were grouped in bins of size 0.2 for LOGIK, 1.00D for K_{max} , 0.10mm for posterior radius, 10 μ m for P_{min} , and 0.8 for BAD-D. Although some of the patients showed a symmetric stage of the disease (values close to the diagonal line), asymmetry was more common for all the parameters studied. Despite this asymmetry, there were no significant differences in the stage between OD and OS (Table 5), indicating that KC has no preference for one eye over the other .

KC STAGING AND CORNEAL SHAPE

The elevation in the vertical and horizontal meridians was analyzed (Figure 4). The baseline examinations were classified using LOGIK and the Gullstrand eye model³⁵ was used as the normal reference, assuming a fixed pachymetry of 550 μ m. As expected, advanced stages presented higher deviations from the normal profile for both the anterior and posterior surfaces. Deviations from normality were more pronounced in the vertical than in the horizontal meridian, and inferior slopes were steeper than the superior slopes.

Grouped by LOGIK stage, the natural history of KC was also calculated in the form of average and standard deviation maps of the anterior and posterior elevation, pachymetry and tangential curvature. Clear differences between the different KC stages can be observed, raising the possibility of using these maps as a graphical reference to classify KC (Figure 5).

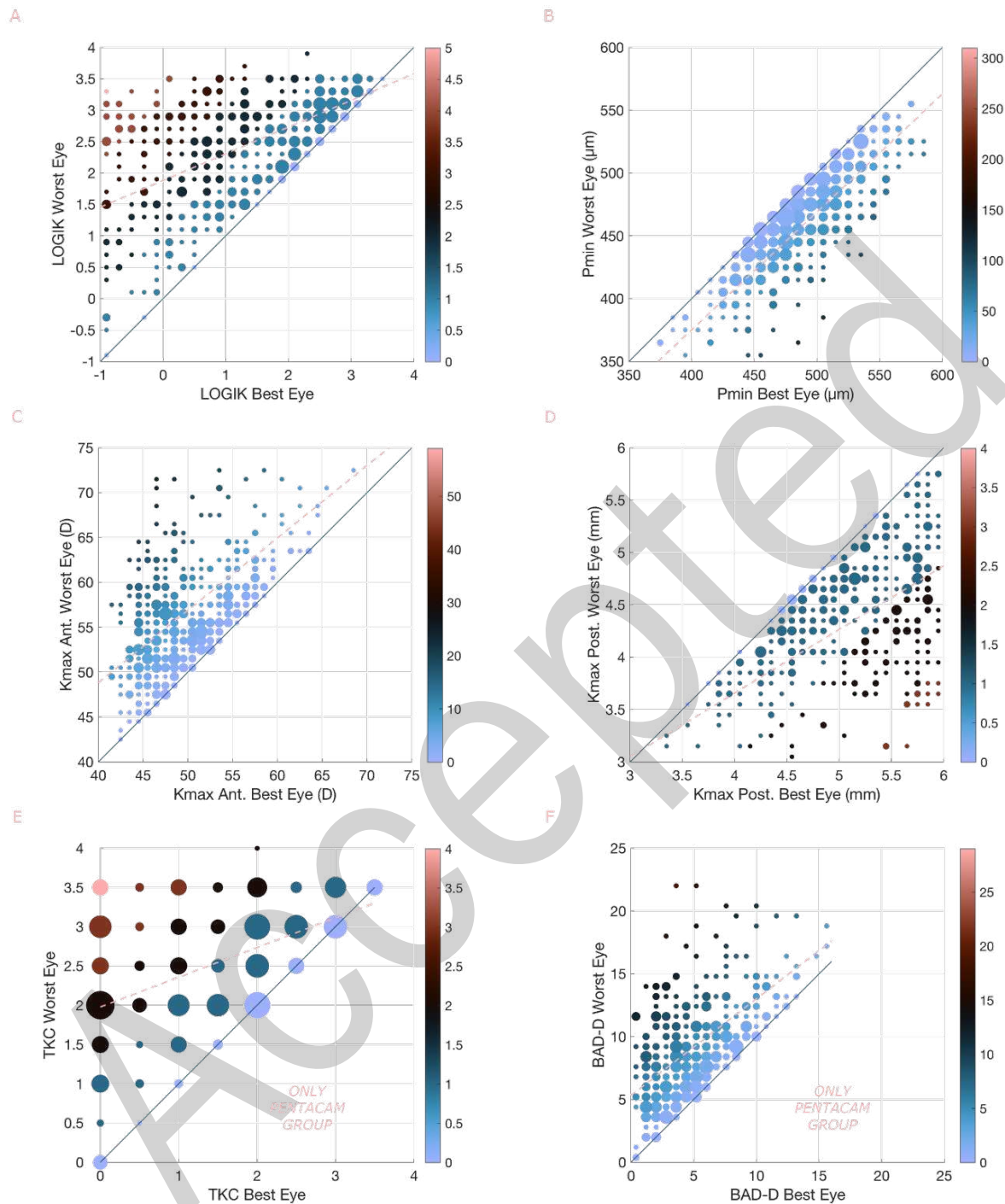


Figure 3. Inter-eye asymmetry. Color represents the inter-eye difference magnitude. **A.** LOGIK (worst eye with higher values). **B.** minimum pachymetry $-P_{min}$ - (worst eye with lower P_{min}). **C.** maximum anterior keratometry $-K_{max}$ - (worst eye with higher K_{max}). **D.** maximum posterior keratometry (worst eye the one with smaller radius). **E.** TKC (only Pentacam, 401 patients; worst eye with higher values). **F.** BAD-D (only Pentacam, 412 patients; worst eye with higher BAD-D).

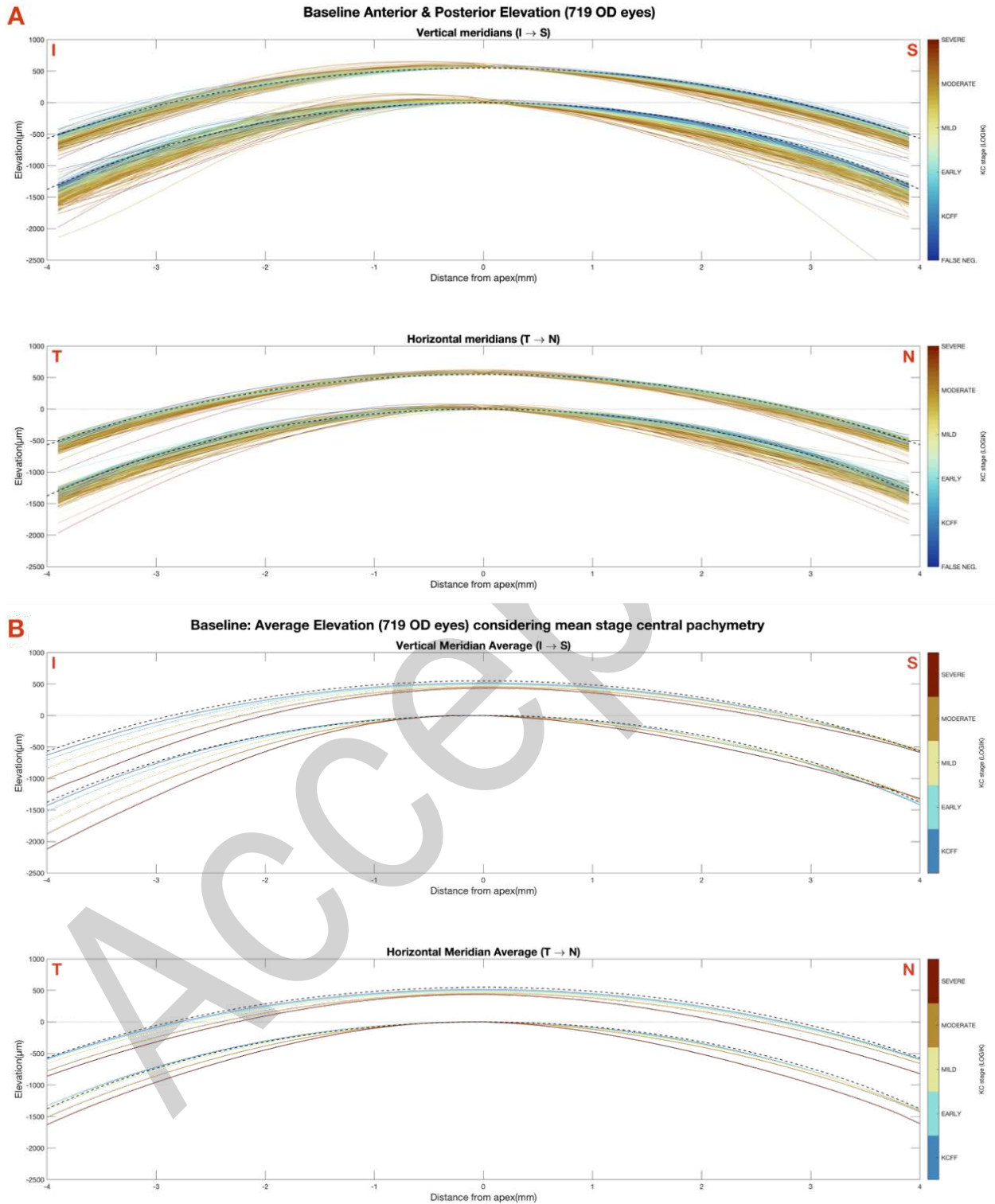


Figure 4. Elevation profiles (719 OD). Reference dashed black line: Gullstrand eye model. **A.** Elevation profiles horizontal and vertical meridians colored by KC stage according to LOGIK. **B.** Average elevation profiles in the horizontal and vertical meridian according to stage. Central pachymetry is the stage average pachymetry.

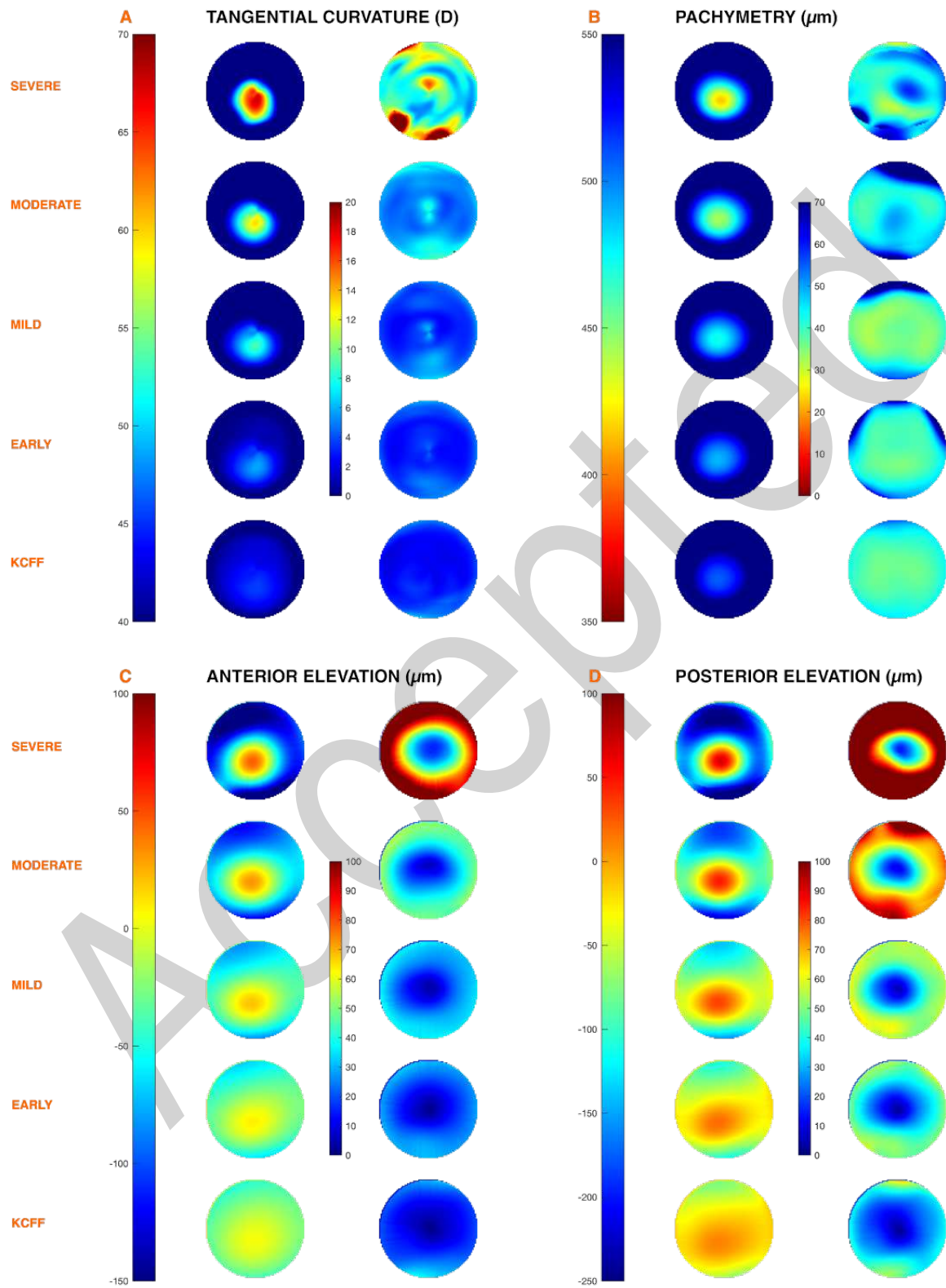


Figure 5. Average (left column) and standard deviation (right column) maps (8 mm diameter) according to LOGIK assigned KC stage **A.** Anterior Tangential Curvature. **B.** Pachymetry. **C.** Anterior Elevation. **D.** Posterior Elevation.

DISCUSSION

The REDCAKE longitudinal study of keratoconic eyes is one of the biggest of its kind since the CLEK Study in the late 90s.³⁶ While the latter relied on classic videokeratography, the current work used state-of-the-art Scheimpflug systems. These corneal tomographers provide information of both the anterior and the posterior corneal surfaces, allowing more insights into the corneal shape.

The REDCAKE cohort displayed a major gender imbalance, with a ratio of almost 3:1 male to female. These percentages were higher than the 60/40 imbalance found in the Netherlands,^{4,37} U.S.A.,³⁶ New Zealand,³⁸ and Turkey.³⁹ In contrast, no sex predisposition was found in South Korea.⁴⁰ Since five European countries and Israel provided REDCAKE data, 75% of the participants were Caucasian and 25% were Asians or Arabs/North Africans.

The novel LOGIK classification system reduced the number of undetected cases and allowed dividing the sample into five KC stages in a way that is more balanced than the one obtained using previous grading systems, such as TKC or ABCD that were used here to classify the Pentacam examinations. The original ABCD classification system was used, as proposed by the authors,⁴¹ even though the constituent ARC and PRC parameters tend to show higher repeatability for KC than the discretized values A and B. (Submitted, Kreps et al. Repeatability of the Pentacam HR in various grades of keratoconus.) Those parameters -PRC and ARC- centered in the P_{\min} point, showed a high correlation. This anterior-posterior correlation was previously reported considering the central curvature.⁴² Previous studies have proposed that abnormalities in the posterior surface might be the first sign of KC.^{25,43} In REDCAKE cohort, alterations in the back surface with no changes in the thickness or the anterior surface (AO B>0 CO) were found in 78 eyes (7%), while 84 eyes (7%) had an abnormal pachymetry without alterations in curvature (AO BO C>0). Two directions of KC evolution might exist: those that start with posterior changes and those that start with an abnormal pachymetry. But it might be also possible that KC is being over-diagnosed based on pachymetry. These special cases will be evaluated in the longitudinal analysis in a future paper.

We also noted that whilst K_{\max} location showed a high variability in this cohort, 94% of the P_{\min} points were located inferotemporally. An inferotemporal position of the thinnest point (0.44mm temporal and 0.29mm inferior on average) was reported previously for normal subjects, with an inferior displacement >1mm found in only 0.5%.⁴⁴ The position of the thinnest point of the cornea presents a characteristic inter-eye symmetry even in KC eyes,^{45,46} and it has been suggested that the displacement of the thinnest point may be happening in the earlier stages of the disease.^{46,47} Additionally, the extent of the asymmetry at baseline examination was quantified for some of the most

common parameters: anterior and posterior K_{max} , LOGIK, TKC, BAD-D, and P_{min} . Although some of the patients showed a symmetric stage of the disease, asymmetry at baseline was more prevalent for all the parameters studied. This asymmetry in KC may play a significant role in the detection, as patients may not present until the second eye is affected.

The tomographies were used to determine the average and standard deviation maps for each KC stage. Leveraging its platform-independency, the examinations were graded using LOGIK classification system, which allowed us to combine Pentacam and Galilei measurements into the computations. This approach is supported by the earlier observation that there are no significant differences in the mean of the Zernike coefficients (up to the 6th level) when fitting elevation maps obtained with both devices⁴⁸. The map set presented may be used as a graphical guidance in KC staging, as well as the elevation profiles provided.

The general limitations of the REDCAKE study should be acknowledged. REDCAKE sample is limited to patients aged between 12 and 40, without ocular or systemic comorbidities and untreated (no CXL applied), which may not correspond with the general KC population. Indirectly, the geographical origin of the data influenced that Caucasians and Middle-Eastern/ North African account for the 99% of the data, while other ethnicities are not represented in the sample. The lack of refraction and slit lamp information should also be considered a limitation, since all conclusions will be based on tomographical data only, excluding the possibility of correlating tomographical changes with clinical signs. BCDVA is not available either, but other studies have shown that BCDVA correlates poorly with the KC severity and is not required to document progression.^{1,49} Finally, there are structural differences between Galilei and Pentacam data that impede performing the exact same analyses for both samples. In the present study, although the average maps and elevation profiles took data from both devices into account, the ones for advanced KC were calculated based on a limited number of eyes while more than one hundred were used for the rest of stages, and this should be taken into consideration since they might be less reliable. Moreover, XY and Z alignment errors, more frequent in advanced cases, might influence the elevation maps; those errors were identified in <0.6% of the exams.

REDCAKE subjects' baseline data analysis is presented here, with a focus on the parameters most often used to describe KC. Based on these data, several previously known properties about KC could be confirmed, and tomographical references for KC stages were presented. Since this is a longitudinal

study with follow-up periods ranging from 5 months to over 10 years, longitudinal data analyses will be presented in future papers.

CONFLICTS OF INTERESTS AND SOURCE OF FUNDING

The authors declare no conflict of interests. This work was supported by a research grant by the Flemish Government Agency for Innovation by Science and Technology (grant no. TBM-T000416N)

ACKNOWLEDGEMENTS

THE REDCAKE STUDY GROUP

EVICR.net European Vision Institute Clinical Research Network,

AIBILI, Azinhaga de Santa Comba, Celas, 3000-548 Coimbra, Portugal.

Centre A- University Medical Center of Johannes Gutenberg-University (Germany)

Katrin Lorenz, Katharina Bell, Anna Beck

Centre B- Ghent University Hospital (Belgium)

Bart Leroy, Elke Kreps

Centre C- Antwerp University Hospital (Belgium)

Jos Rozema, Marta Jiménez-García, Sorcha Ní Dhubhghaill, Ikram Issarti, Alejandra Consejo, Carina Koppen

Centre D- Fondation Asile des Aveugles, Jules Gonin Eye Hospital (Switzerland)

Kattayoon Hashemi

Centre E- University Eye Clinic Maastricht (The Netherlands)

Rudy MMA Nuijts, Magali Vandevenne, Frank JHM van den Biggelaar

Centre F- Braga Hospital (Portugal)

Tiago Monteiro, Rui Freitas

Centre H- Justus Liebig University Giessen (Germany)

Birgit Lorenz, Ekaterina Sokolenko, Francesco Luciani, Christine Mais

Centre I-Tel Aviv Sourasky Medical Center (Israel)

David Varssano, Eyal Cohen

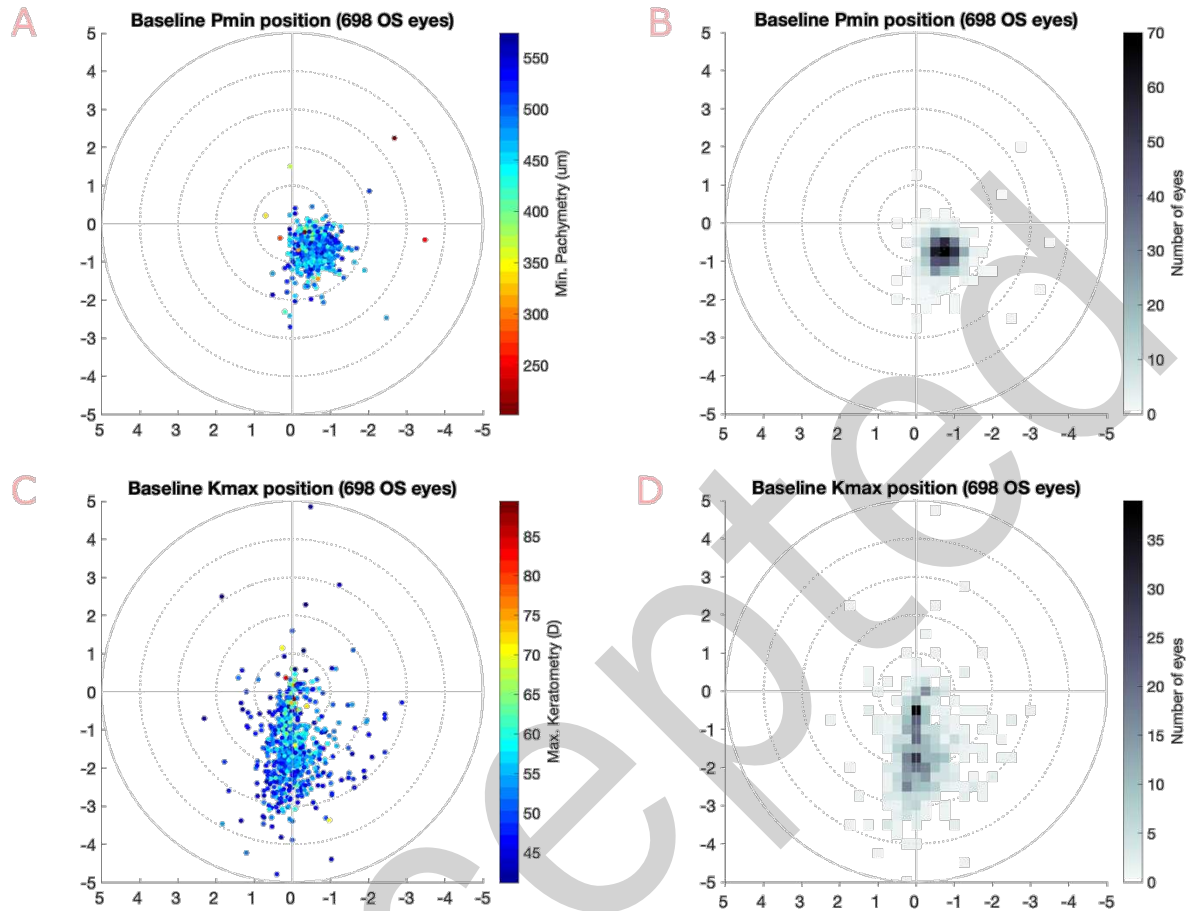
REFERENCES

1. Gomes JAP, Tan D, Rapuano CJ, et al. Global Consensus on Keratoconus and Ectatic Diseases. *Cornea*. 2015;34:359-369. doi:10.1097/ICO.0000000000000408.
2. Rabinowitz YS. Keratoconus. *Surv Ophthalmol*. 1998;42:297-319. doi:10.1016/S0039-6257(97)00119-7.
3. Rozema JJ, Zakaria N, Hidalgo IR, et al. How abnormal is the noncorneal biometry of keratoconic eyes? *Cornea*. 2016;35:860-865. doi:10.1097/ICO.0000000000000802.
4. Godefrooij DA, de Wit GA, Uiterwaal CS, et al. Age-specific Incidence and Prevalence of Keratoconus: A Nationwide Registration Study. *Am J Ophthalmol*. 2017;175:169-172. doi:10.1016/j.ajo.2016.12.015.
5. Bawazeer AM. Atopy and keratoconus: a multivariate analysis. *Br J Ophthalmol*. 2000;84:834-836. doi:10.1136/bjo.84.8.834.
6. Gatinel D. Eye rubbing, a sine Qua Non for Keratoconus? *Int J Keratoconus Ectatic Corneal Dis*. 2016;5:6-12. doi:10.5005/jp-journals-10025-1114.
7. Nielsen K, Hjortdal J, Pihlmann M, et al. Update on the keratoconus genetics. *Acta Ophthalmol*. 2013;91:106-113. doi:10.1111/j.1755-3768.2012.02400.x.
8. Wang Y, Rabinowitz YS, Rotter JI, et al. Genetic epidemiological study of keratoconus: Evidence for major gene determination. *Am J Med Genet*. 2000;93:403-409. doi:10.1002/1096-8628(20000828)93:5<403::AID-AJMG11>3.0.CO;2-A.
9. Marchitti SA, Chen Y, Thompson DC, et al. Ultraviolet Radiation: Cellular Antioxidant Response and the Role of Ocular Aldehyde Dehydrogenase Enzymes. *Eye Contact Lens Sci Clin Pract*. 2011;37:206-213. doi:10.1097/ICL.0b013e3182212642.
10. Galletti JD, Ruiseñor Vázquez PR, Minguez N, et al. Corneal Asymmetry Analysis by Pentacam Scheimpflug Tomography for Keratoconus Diagnosis. *J Refract Surg*. 2015;31:116-123. doi:10.3928/1081597X-20150122-07.
11. Goebels S, Eppig T, Seitz B, et al. [Intraindividual Keratoconus Progression]. *Klin Monbl Augenheilkd*. 2017;234:1010-1014. doi:10.1055/s-0043-106300.
12. Li X, Rabinowitz YS, Rasheed K, et al. Longitudinal study of the normal eyes in unilateral keratoconus patients. *Ophthalmology*. 2004;111:440-446. doi:10.1016/j.ophtha.2003.06.020.
13. Shirayama-Suzuki M, Amano S, Honda N, et al. Longitudinal analysis of corneal topography in suspected keratoconus. *Br J Ophthalmol*. 2009;93:815-819. doi:10.1136/bjo.2008.140012.
14. Klyce SD. Chasing the suspect: keratoconus. *Br J Ophthalmol*. 2009;93:845-847. doi:10.1136/bjo.2008.147371.
15. Ambrósio R, Faria-Correia F, Silva-Lopes I, et al. Evolution on Keratoconus and Corneal Ectatic Diseases Paradigms and Paradoxes. *Int J Keratoconus Ectatic Corneal Dis*. 2018;7:35-49.
16. Romano V, Vinciguerra R, Arbabi EM, et al. Progression of Keratoconus in Patients While Awaiting Corneal Cross-linking: A Prospective Clinical Study. *J Refract Surg*. 2018;34:177-180. doi:10.3928/1081597X-20180104-01.
17. Koppen C, Kreps EO, Anthonissen L, et al. Scleral Lenses Reduce the Need for Corneal Transplants in Severe Keratoconus. *Am J Ophthalmol*. 2018;185:43-47. doi:10.1016/j.ajo.2017.10.022.
18. Kreps EO, Claerhout I, Koppen C. The Outcome of Scleral Lens Fitting for Keratoconus with Resolved Corneal Hydrops. *Cornea*. 2019;38:855-858. doi:10.1097/ICO.0000000000001946.
19. Raiskup F, Theuring A, Pillunat LE, et al. Corneal collagen crosslinking with riboflavin and ultraviolet-A light in progressive keratoconus: Ten-year results. *J Cataract Refract Surg*. 2015;41:41-46. doi:10.1016/j.jcrs.2014.09.033.

20. Alió JL, Piñero DP, Alesón A, et al. Keratoconus-integrated characterization considering anterior corneal aberrations, internal astigmatism, and corneal biomechanics. *J Cataract Refract Surg.* 2011;37:552-568. doi:10.1016/j.jcrs.2010.10.046.
21. Ambrósio R, Alonso RS, Luz A, et al. Corneal-thickness spatial profile and corneal-volume distribution: tomographic indices to detect keratoconus. *J Cataract Refract Surg.* 2006;32:1851-1859. doi:10.1016/j.jcrs.2006.06.025.
22. Ambrósio R, Caiado Canedo AL, Guerra FP, et al. Novel pachymetric parameters based on corneal tomography for diagnosing keratoconus. *J Refract Surg.* 2011;27:753-758. doi:10.3928/1081597X-20110721-01.
23. Reeves SW, Stinnett S, Adelman RA, et al. Risk Factors for Progression to Penetrating Keratoplasty in Patients With Keratoconus. *Am J Ophthalmol.* 2005;140:607.e1-607.e6. doi:10.1016/j.ajo.2005.05.029.
24. Hamilton A, Wong S, Carley F, et al. Tomographic indices as possible risk factors for progression in pediatric keratoconus. *J AAPOS Off Publ Am Assoc Pediatr Ophthalmol Strabismus.* 2016;20:523-526. doi:10.1016/j.jaapos.2016.08.006.
25. Tellouck J, Touboul D, Santhiago MR, et al. Evolution Profiles of Different Corneal Parameters in Progressive Keratoconus. *Cornea.* 2016;35:807-813. doi:10.1097/ICO.0000000000000833.
26. Tuft SJ, Moodaley LC, Gregory WM, et al. Prognostic Factors for the Progression of Keratoconus. *Ophthalmology.* 1994;101:439-447. doi:10.1016/S0161-6420(94)31313-3.
27. Lenk J, Spoerl E, Stalder T, et al. Increased Hair Cortisol Concentrations in Patients With Progressive Keratoconus. *J Refract Surg.* 2017;33:383-388. doi:10.3928/1081597X-20170413-01.
28. Piñero DP, Alió JL, Tomás J, et al. Vector analysis of evolutive corneal astigmatic changes in keratoconus. *Investig Ophthalmol Vis Sci.* 2011;52:4054-4062. doi:10.1167/iovs.10-6856.
29. Leoni-Mesplie S, Mortemousque B, Touboul D, et al. Scalability and Severity of Keratoconus in Children. *Am J Ophthalmol.* 2012;154:56-62.e1. doi:10.1016/j.ajo.2012.01.025.
30. Ferdi AC, Nguyen V, Gore DM, et al. Keratoconus Natural Progression. *Ophthalmology.* 2019;126:935-945. doi:10.1016/j.ophtha.2019.02.029.
31. Naderan M, Jahanrad A. Topographic, tomographic and biomechanical corneal changes during pregnancy in patients with keratoconus: a cohort study. *Acta Ophthalmol.* 2017;95:e291-e296. doi:10.1111/aos.13296.
32. Yuksel E, Yalinbas D, Aydin B, et al. Keratoconus Progression Induced by In Vitro Fertilization Treatment. *J Refract Surg.* 2016;32:60-63. doi:10.3928/1081597X-20151207-10.
33. Martínez-Abad A, Piñero DP, Martínez-Abad A, et al. New perspectives on the detection and progression of keratoconus. *J Cataract Refract Surg.* 2017;43:1213-1227. doi:10.1016/j.jcrs.2017.07.021.
34. Evans JD. *Straightforward Statistics for Thebehavioral Sciences.* (Pacific Grove : Brooks/Cole Pub. Co., ed.). Pacific Grove, CA: Brooks/ColePublishing.; 1996.
35. LeGrand Y, ElHage S. *Physiological Optics.* Springer; 1980.
36. Zadnik K, Barr JT, Edrington TB, et al. Baseline findings in the collaborative longitudinal evaluation of keratoconus (CLEK) study. *Invest Ophthalmol Vis Sci.* 1998;39:2537-2546.
37. Wisse RPL, Simons RWP, Van Der Vossen MJB, et al. Clinical Evaluation and Validation of the Dutch Crosslinking for Keratoconus Score. *JAMA Ophthalmol.* 2019;137:610-616. doi:10.1001/jamaophthalmol.2019.0415.
38. Owens H, Gamble G. A profile of keratoconus in New Zealand. *Cornea.* 2003;22:122-125. doi:10.1097/00003226-200303000-00008.
39. Ertan A, Muftuoglu O. Keratoconus Clinical Findings According to Different Age and Gender Groups. *Cornea.* 2008;27:1109-1113. doi:10.1097/ICO.0b013e31817f815a.
40. Hwang S, Lim DH, Chung TY. Prevalence and Incidence of Keratoconus in South Korea: A Nationwide Population-

- based Study. *Am J Ophthalmol*. 2018;192:56-64. doi:10.1016/j.ajo.2018.04.027.
41. Belin MW, Duncan J, Ambrósio R, et al. A new Tomographic Method of Staging/ Classification of Keratoconus :The ABCD Grading System. *Int J Keratoconus Ectatic Corneal Dis*. 2015;4:85-93. doi:10.5005/jp-journals-10025-1105.
 42. Montalbán R, Alió JL, Javaloy J, et al. Correlation of anterior and posterior corneal shape in keratoconus. *Cornea*. 2013;32:916-921. doi:10.1097/ICO.0b013e3182904950.
 43. de Sanctis U, Loiacono C, Richiardi L, et al. Sensitivity and Specificity of Posterior Corneal Elevation Measured by Pentacam in Discriminating Keratoconus/Subclinical Keratoconus. *Ophthalmology*. 2008;115:1534-1539. doi:10.1016/j.ophtha.2008.02.020.
 44. Feng MT, Kim JT, Ambrósio R, et al. International Values of Central Pachymetry in Normal Subjects by Rotating Scheimpflug Camera. *Asia-Pacific J Ophthalmol*. 2012;1:13-18. doi:10.1097/apo.0b013e31823e58da.
 45. Henriquez MA, Izquierdo L, Mannis MJ. Intereye asymmetry detected by scheimpflug imaging in subjects with normal corneas and keratoconus. *Cornea*. 2013;32:779-782. doi:10.1097/ICO.0b013e31827b14ae.
 46. Saad A, Guilbert E, Gatinel D. Corneal enantiomorphism in normal and keratoconic eyes. *J Refract Surg*. 2014;30:542-547. doi:10.3928/1081597X-20140711-07.
 47. Saad A, Gatinel D. Topographic and Tomographic Properties of Forme Fruste Keratoconus Corneas. *Invest Ophthalmol Vis Sci*. 2010;51:5546. doi:10.1167/iovs.10-5369.
 48. De Jong T, Sheehan MT, Dubbelman M, et al. Shape of the anterior cornea: Comparison of height data from 4 corneal topographers. *J Cataract Refract Surg*. 2013;39:1570-1580. doi:10.1016/j.jcrs.2013.04.032.
 49. Kanellopoulos AJ, Asimellis G. Revisiting keratoconus diagnosis and progression classification based on evaluation of corneal asymmetry indices, derived from Scheimpflug imaging in keratoconic and suspect cases. *Clin Ophthalmol*. 2013;7:1539-1548. doi:10.2147/OPHT.S44741.

SUPPLEMENTAL DIGITAL CONTENT



Supplemental Digital Content 1. Minimum corneal pachymetry (P_{min}) and maximum anterior keratometry (K_{max}) at baseline examination for 698 OS eyes. Axes: distance from corneal center (mm) **A.** Location of P_{min} . Colour scale related to pachymetry value. **B.** Frequency heatmap graph for the location of P_{min} . **C.** Location of K_{max} . Color scale related to keratometry value. **D.** Frequency heatmap graph for the location of K_{max} .